

THE X-RAY EMISSION FROM THE NUCLEUS OF THE DWARF ELLIPTICAL GALAXY
NGC 3226

I.M. GEORGE^{1,2}, R.F. MUSHOTZKY¹, T. YAQOUB^{1,3}, T.J. TURNER^{1,2}, S. KRAEMER^{4,5}, A.F. PTAK⁶,
K. NANDRA^{1,7}, D.M. CRENSHAW^{4,5}, H. NETZER⁸

Accepted for publication in The Astrophysical Journal

ABSTRACT

We present the first high resolution X-ray image of the dwarf elliptical galaxy NGC 3226. The data were obtained during an observation of the nearby Seyfert Galaxy NGC 3227 using the *Chandra X-ray Observatory*. We detect a point X-ray source spatially consistent with the optical nucleus of NGC 3226 and a recently-detected, compact, flat-spectrum, radio source. The X-ray spectrum can be measured up to ~ 10 keV and is consistent with a power law with a photon index $1.7 \lesssim \Gamma \lesssim 2.2$, or thermal bremsstrahlung emission with $4 \lesssim kT \lesssim 10$ keV. In both cases the luminosity in the 2–10 keV band $\simeq 10^{40} h_{75}^{-1}$ erg s⁻¹. We find marginal evidence that the nucleus varies within the observation. These characteristics support evidence from other wavebands that NGC 3226 harbors a low-luminosity, active nucleus. We also comment on two previously-unknown, fainter X-ray sources $\lesssim 15$ arcsec from the nucleus of NGC 3226. Their proximity to the nucleus (with projected distances $\lesssim 1.3 h_{75}^{-1}$ kpc) suggests both are within NGC 3226, and thus have luminosities ($\sim \text{few} \times 10^{38}$ – $\text{few} \times 10^{39}$ erg s⁻¹) consistent with black-hole binary systems.

Subject headings: galaxies: dwarf – galaxies: active – galaxies: individual (NGC 3226) – galaxies: nuclei – X-rays: galaxies – X-rays: binaries

1. INTRODUCTION

NGC 3226 is a dwarf elliptical galaxy ($z = 0.00441 \pm 0.00006$; e.g. de Vaucouleurs et al. 1991) interacting with the nearby SAB(s)a galaxy NGC 3227⁹. The center of NGC 3226 hosts a low-ionization nuclear emission-line region (LINER) of optical spectroscopic type 1.9 (Ho, Filipenko & Sargent, 1997a), along with large quantities of dust in filamentary structures (e.g. Rest et al. 2001). A compact, flat-spectrum radio source has recently been detected (Nagar et al. 2000; Falcke et al. 2000) at a location consistent with the optical nucleus. This, along with the claim of a broad component to the H α emission line (FWHM $\sim 2 \times 10^3$ km s⁻¹; Ho et al. 1997b), suggests the galaxy hosts an active galactic nucleus (AGN) rather than a region of aging starburst activity. The luminosity of the broad H α line in NGC 3226 ($L(\text{H}\alpha) \simeq 10^{39}$ erg s⁻¹) is an order of magnitude below the dividing line between so-called low-luminosity AGN (LLAGN, or “dwarf” Seyfert galaxies) and the more powerful (“normal”) Seyfert 1 and giant elliptical galaxies.

X-ray emission from the nuclear regions of NGC 3226 has been detected using both the *ROSAT*PSPC (Komossa & Fink 1997; Sansom, Hibbard & Schweizer 2000) and

HRI (Roberts & Warwick 2000) with an implied luminosity $L(0.1\text{--}2 \text{ keV}) \sim 10^{40}$ erg s⁻¹. However these data sets had relatively poor spatial resolution, and were unable to distinguish either spatially or spectroscopically between an (AGN-like) power law X-ray spectrum and a collisionally ionized plasma due to hot gas (e.g. from a starburst region).

In this *Letter* we present results for NGC 3226 obtained using the *Chandra X-ray Observatory* (*CXO*; e.g. Weiskopf, O’Dell, van Speybroeck 1996). Following a brief description of the observation (§2), in §3 we report the detection of three X-ray sources within the inner ~ 2 kpc of the nucleus, with brightest source identified as the nucleus of NGC 3226. In §4 we report the temporal and spectral characteristics of the nucleus, and discuss the evidence that NGC 3226 harbors a LLAGN. The limited constraints that can be obtained from the two off-nuclear sources are discussed in §5. We present our conclusions in §6.

2. THE OBSERVATION

The data from NGC 3226 reported here were obtained during an observation using the *CXO* in 1999 Dec. The High Energy Transmission Grating Spectrometer (HETGS; e.g.

¹ Laboratory for High Energy Astrophysics, Code 662, NASA/Goddard Space Flight Center, Greenbelt, MD 20771

² Joint Center for Astrophysics, Department of Physics, University of Maryland, Baltimore County, 1000 Hilltop Circle, Baltimore, MD 21250

³ Department of Physics & Astronomy, Johns Hopkins University, 3400 North Charles Street, Baltimore, MD 21218

⁴ Laboratory for Astronomy and Solar Physics, Code 681, NASA/Goddard Space Flight Center, Greenbelt, MD 20771

⁵ Institute for Astrophysics and Computational Sciences, The Catholic University of America, Washington D.C. 20064

⁶ Department of Physics, Carnegie Mellon University, Pittsburgh, PA 15213

⁷ Universities Space Research Association

⁸ School of Physics and Astronomy and the Wise Observatory, The Beverly and Raymond Sackler Faculty of Exact Sciences, Tel Aviv University, Tel Aviv 69978, Israel.

⁹ For simplicity, here we use the heliocentric velocity (1322 ± 19 km s⁻¹) measured using optical emission lines to derive the distance to NGC 3226. Given its interaction with NGC 3227 (1157 ± 3 km s⁻¹), the distance may be slightly over-estimated (by $\lesssim 14\%$), but this does not affect any of the conclusions presented here.

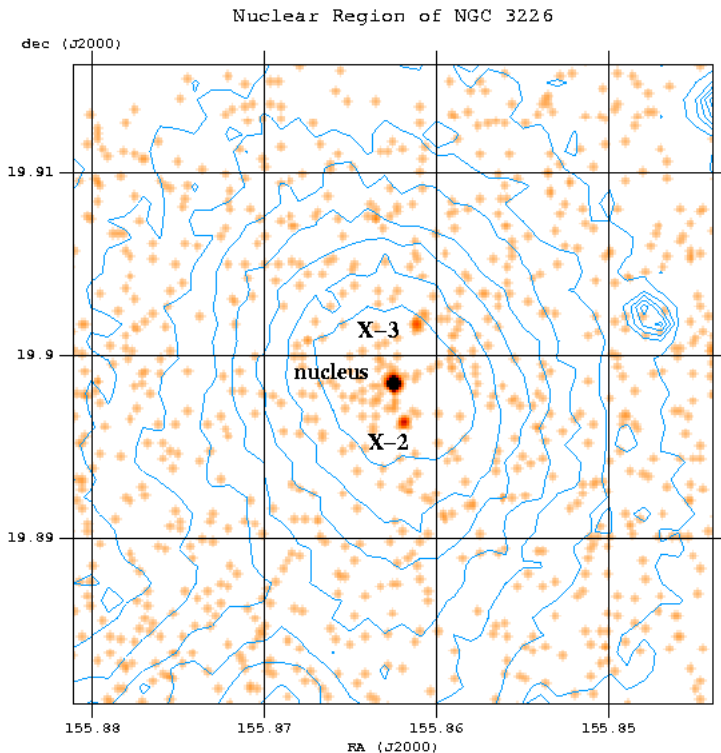


FIG. 1.— The 0th-order HETGS image of the nuclear region of NGC 3226 in the 0.8-6 keV band. For clarity the image has been smoothed by a Gaussian with $\sigma = 0.492$ arcsec. The DSS image is overlaid as the blue, linearly-spaced contours. The separation between the grid lines (10^{-2} degrees) $\simeq 3.1h_{75}^{-1}$ kpc. The offsets between the position of the brightest X-ray source and the optical nucleus of NGC 3226 as tabulated by Cotton, Condon & Arbizzani (1999) are $(\Delta\text{RA}, \Delta\text{dec}) = (-1.2 \text{ arcsec}, +0.2 \text{ arcsec})$. Currently there are no optical identifications of the other two X-ray sources (marked X-2 & X-3).

Markert et al. 1994) was employed with the Advanced CCD Imaging Spectrometer (ACIS; e.g. Nousek et al 1998) in the focal plane (with a temperature of -110°C). The HETGS consists of two sets of gratings (hereafter the medium- and high-energy grating {MEG & HEG} “arms”), each with a different period and intercepting X-rays from (two of the four) different shells of the X-ray telescope. The rulings of the MEG and HEG differ by ~ 10 degrees preventing any spatial overlap in the dispersed spectra of an on-axis, point source. The ACIS-S array was placed at the optical axis, consisting of 6 CCD chips¹⁰ orientated to record the undispersed (0th-order) photons from the target and nearby sources (on the ACIS-S3 CCD), along with both the positive and negative orders of the spectrum dispersed by both grating arms of the HETGS.

The observation was continuous, with a total duration of 49.9 ks. Following screening and removing the “streaks” from the s4 chip using `dstreak` (v 1.3; Houck 2000), the resultant exposure time was 46.3 ks. All the data analysis presented here was performed using the *Chandra* CALDB (v2.0), and the CIAO (v2.0.2) and HEASoft (v5.0.2) software packages. Further details on the instrumental parameters and the data reduction can be found in George et al. (2001), along with the scientific results for NGC 3227.

3. SPATIAL ANALYSIS

In Fig. 1 we show an image of NGC 3226 in the 0.6-8 keV band. For simplicity, here we ignore any peculiar motion associated with the NGC 3226/3227 system or other members of its local group, and simply use the heliocentric velocity of NGC 3226 to derive a distance to $17.6h_{75}^{-1}$ Mpc (where $h_{75} = H_0/75 \text{ km s}^{-1} \text{ Mpc}^{-1}$). Thus $1 \text{ arcsec} \equiv 85h_{75}^{-1} \text{ pc}$. Three X-ray sources are evident. We find the centroid of the brightest source to be at RA=10h 23m 27.00s, dec=+19d 53m 54.7s (J2000). This is consistent the position of the optical nucleus of NGC 3226 (RA=10h 23m 27.08s, dec=+19d 53m 54.5s; Cotton, Condon & Arbizzani 1999) within the current uncertainties in the aspect reconstruction of *CXO* data ($\lesssim 1 \text{ arcsec}$; Aldcroft, p.comm), and in excellent agreement with the compact, flat-spectrum radio source (RA=10h 23m 27.01s, dec=+19d 53m 54.5s; Falcke et al. 2000). Thus we identify this X-ray emission as the HETGS 0th-order image of the inner $\sim 150h_{75}^{-1} \text{ pc}$ of NGC 3226. From an analysis using a Marr wavelet function provided by the `wavdetect` task in CIAO we estimate a net source count rate of $491 \pm 22 \text{ count s}^{-1}$.

To the best of our knowledge, nothing has been reported in the literature concerning the other two sources, CXO J102334.1+195347 and CXO J102326.7+195407 (labelled X-2 & X-3 respectively in Fig. 1). Both are much weaker than the nucleus (with estimated source count rates of $20 \pm 5 \text{ count s}^{-1}$ and $18 \pm 4 \text{ count s}^{-1}$ respectively).

¹⁰ The ACIS-S0 chip was not in operation during the observation due to instrumental concerns.

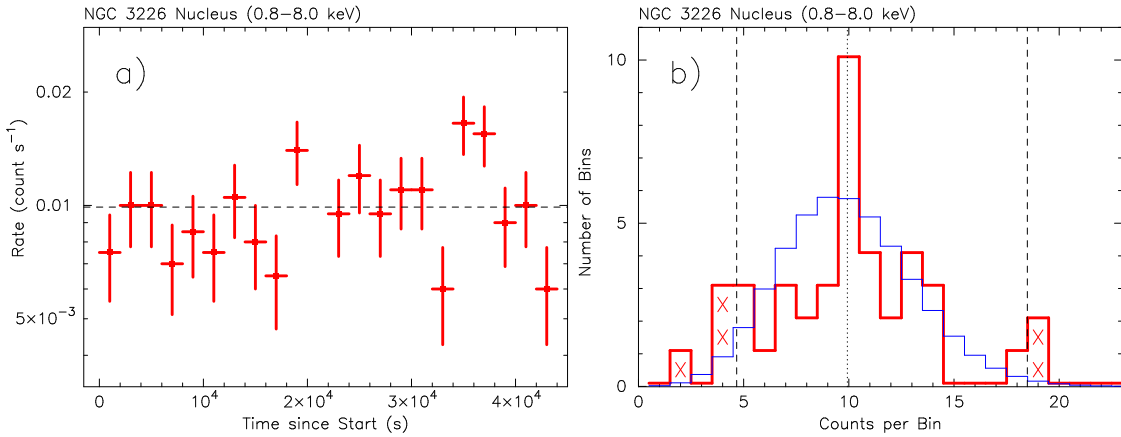


FIG. 2.— a) A light curve of the nucleus of NGC 3226 in the 0.8–6 keV band using 2×10^3 s bins. Note that the y-axis is logarithmic, with a dynamic range 0.33–3.0 times the mean count rate (0.0099 ct s^{-1} ; dashed line). The predicted background rate is $\simeq 3 \times 10^{-5} \text{ count s}^{-1}$ and constant. b) Observed distribution (red) of number of bins (each of 10^3 s) containing n counts, and a Poisson distribution (blue) derived from the mean count rate. The dashed lines show the 95% confidence limits for the Poisson distribution. The bins marked with an “X” highlight more bins are observed outside these limits than predicted.

4. THE NUCLEUS OF NGC 3226

For the (temporal and spectral analysis) presented below we employed a circular extraction cell of radius $\simeq 2.5$ arcsec centered on the nucleus. The background was obtained from a circular annulus with an outer radius $\simeq 25$ arcsec centered on the nucleus, but also excluding circular regions of radius $\simeq 2.5$ arcsec around X-2 and X-3. The background was then rescaled to be appropriate for the source extraction cell.

4.1. Temporal Variability

We find marginal evidence for variability from the nucleus of NGC 3226. In Fig. 2a we show the observed count rate in 0.8–6 keV band as a function of time using 2×10^3 s bins. There are 21 such bins, each containing ~ 20 counts on average, thus χ^2 -statistics can be used (but with some caution). The hypothesis of a constant count rate is rejected at $\sim 94\%$ confidence ($\chi^2_\nu = 1.53$ for 20 degrees of freedom, hereafter d.o.f.). Using 4×10^3 s bins, a constant count rate is rejected at $\sim 97\%$ confidence ($\chi^2_\nu = 1.96$ for 10 d.o.f.).

Given the data from NGC 3226 are in the “grey-area” where the appropriateness of using χ^2 -statistics is debatable (i.e. $\lesssim 20$ bins, each with a relatively small number of counts) we have also performed a temporal analysis assuming Poissonian statistics. This analysis also indicates evidence for variability. For example, in Fig. 2b we show the observed (red) number of bins (each of 10^3 s), containing 0, 1, 2, ... counts compared to the predicted Poisson distribution (blue) derived from the mean count rate of $\simeq 0.01 \text{ ct s}^{-1}$. For the example shown, we find 6 of the 42 bins outside the the 95% confidence limits (dashed lines in Fig. 2b) compared to the 2.1 predicted from a Poisson distribution. We have repeated this analysis 20 times, on each occasion offsetting the start time of each 10^3 s bin by $1/20$ of a bin width. We find the observed number of bins exceeds the predicted number on 13 of the 20 occasions. Similarly we have repeated the analysis using bins of different temporal sizes, and find cases where number of bins observed outside the 95% confidence limits exceeds that expected for bins in the $\sim \text{few} \times 10^2$ – $\text{few} \times 10^3$ s. Neverthe-

less, given the current data are in the Poissonian regime, again we consider the evidence only marginal.

4.2. Spectral Analysis

Spectra were extracted from the (0th-order) cell described above using the `psextract` script in `CIAO`. The resultant Pulse-Invariant (PI) channels at energies > 0.5 keV were then grouped so as to contain a minimum of 20 counts per bin, and hence allowing a χ^2 minimization technique to be employed. This resulted in 24 spectral bins which were analyzed within the `XSPEC` (v 11.0.1) package. For the Galactic absorption along the line-of-sight we assume an effective hydrogen column density of $N_{HI}^{gal} = 2.08 \times 10^{20} \text{ cm}^{-2}$ (as measured towards NGC 3227; Murphy et al 1996).

We find an absorbed power law provides an adequate fit to the data ($\chi^2 = 20.1$ for 21 degrees of freedom). The best-fitting parameters and 68% confidence ranges are a photon index $\Gamma = 1.94^{+0.26}_{-0.25}$, and intrinsic absorption (in addition to N_{HI}^{gal}) of $N_H = (4.8^{+1.7}_{-1.5}) \times 10^{21} \text{ cm}^{-2}$. The implied luminosity (corrected for absorption) in the 0.4–10 keV band is $L(0.4\text{--}10 \text{ keV}) \simeq 3.5^{+1.4}_{-1.0} \times 10^{40} h_{75}^{-1} \text{ erg s}^{-1}$, and that in the 2–10 keV band $L(2\text{--}10 \text{ keV}) \simeq 1.8^{+0.8}_{-0.3} \times 10^{40} h_{75}^{-1} \text{ erg s}^{-1}$. The data and this model are shown in Fig. 3a. Unfortunately any Fe $K\alpha$ emission cannot be well constrained by the data (equivalent widths $EW \lesssim 0.9$ keV and $\lesssim 1.5$ keV for narrow and broad lines at 6.4 keV respectively). An absorbed thermal bremsstrahlung also provides an adequate fit to the data ($\chi^2 = 22.2$ for 21 degrees of freedom), with $kT = 6.5^{+4.4}_{-2.1}$ keV, and with a luminosity and N_H (in addition to N_{HI}^{gal}) consistent with those found above. We shall discuss these two models further in §4.3.

The nucleus of NGC 3226 is sufficiently bright to also be detected in the dispersed spectrum. Source and background spectra were extracted using the procedure described in George et al. (2001). The source exceeds the mean background level in the $\pm 1^{\text{st}}$ -orders in the ranges 0.18–1.7 nm (MEG) and 0.15–1.0 nm (HEG). The spectral resolution of the MEG and HEG can be well approximated by Gaussians with (“ 1σ ”) widths $\simeq 1$ pm and $\simeq 0.5$ pm

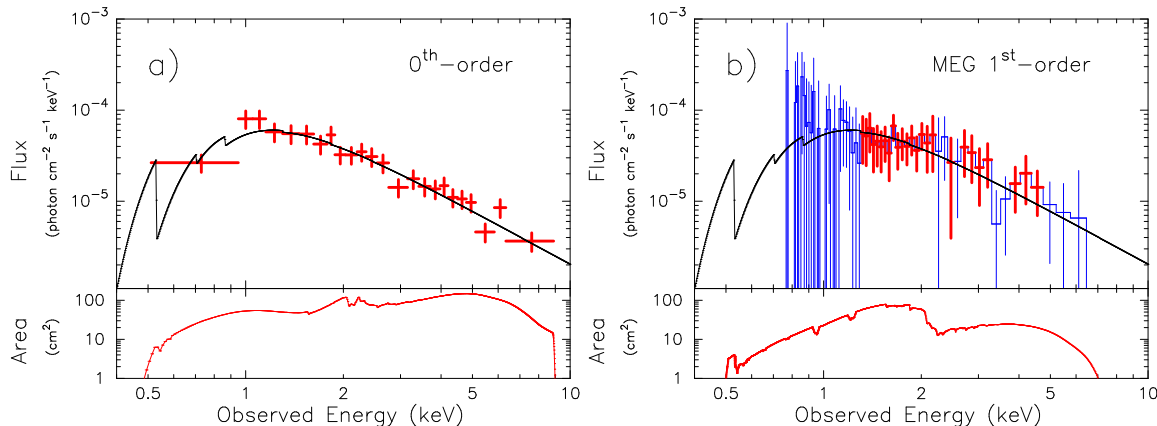


FIG. 3.— The upper panels show the spectra from the nucleus of NGC 3226, along with the absorbed, power-law model discussed in the text. Bins which contain more than 1 photon at $> 97.5\%$ confidence are shown in red. The lower panels show the effective area of the instruments. a) The 0^{th} -order spectrum grouped such that each bin contains ≥ 20 counts. b) The MEG 1^{st} -order spectrum derived using only data < 1.6 nm (-1^{st} -order) and < 1.8 nm ($+1^{\text{st}}$ -order) to maximize the signal-to-noise ratio. For clarity the data are shown using 23 pm wide bins (ie. $10\times$ the FWHM of the MEG spectral resolution). No statistically significant features are present in the spectrum made at the full MEG resolution.

respectively ($1 \text{ pm} \equiv 10^{-12} \text{ m}$; and also corresponds to ~ 1 ACIS pixel¹¹). Both the MEG and HEG spectra have a very low signal-to-noise ratio ($\lesssim 0.5 \text{ ct pm}^{-1}$ and $\gtrsim 0.3 \text{ ct pm}^{-1}$ respectively). We have constructed spectra using bins between 1 and 4 times the resolution of each grating arm. However we find no cases where the number of counts per bin exceeds 7 ($\simeq 99\%$ confidence limit for 1 count per bin), and hence no evidence that the spectrum contains any intense emission lines. Using larger bin sizes, we find both the MEG and HEG spectra are in good agreement with that derived from the 0^{th} -order (e.g. Fig.3b). Thus we find no requirement for additional spectral complexity from either the 0^{th} -order or dispersed spectra.

Our spectral models predict *ROSATHRI* count rates ($\sim 4 \times 10^{-3} \text{ ct s}^{-1}$) consistent with those seen during an observation in 1995 Aug (Roberts & Warwick 2000). However the predicted *ROSAT* PSPC count rates ($\sim 10^{-2} \text{ ct s}^{-1}$) are slightly lower than that reported during an observation in 1993 May ($\sim 4 \times 10^{-2} \text{ ct s}^{-1}$ from within a circular region of radius $\sim 15h_{75}^{-1} \text{ kpc}$ is reported by Sansom et al. 2000). This may be the result of variability on long timescales, and/or an additional soft X-ray component from the AGN. However at least part of the higher count rate seen by the PSPC may be due to other sources of (perhaps time-variable) X-ray emission associated with the galaxy.

4.3. The Case for a LLAGN at the Center of NGC 3226

The improved spatial resolution of *CXO* has enabled us to show that the X-ray emission from NGC 3226 is dominated by a point-like (tentatively variable) source within $\sim 0.2h_{75}^{-1} \text{ kpc}$ of the nucleus. The X-ray spectrum is measured up to $\sim 10 \text{ keV}$ and is consistent with a power law with a photon index $1.7 \lesssim \Gamma \lesssim 2.2$, or thermal bremsstrahlung emission with $4 \lesssim kT \lesssim 10 \text{ keV}$. The ratio of observed flux at 2 keV ($\simeq 4 \times 10^{-2} \mu\text{Jy}$) to that at 5 GHz from the flat-spectrum, compact radio source (Falcke et al. 2000) gives a radio-to-X-ray spectral index $\alpha_{rx} = -\log(f(2 \text{ keV})/f(5 \text{ GHz}))/7.986 = 0.62$. Such a

value is consistent with that derived from several similar objects, including M 81 (NGC 3031) and NGC 4579 (both with $\alpha_{rx} \simeq 0.6$; e.g. Ho 1999, and references therein). M 81 and NGC 4579 are of note since both are commonly believed to be accretion-powered objects. Indeed Fe $K\alpha$ emission has been detected from both objects, which is broad in the case of M 81 (Ishisaki et al. 1996) and variable in the case of NGC 4579 (Terashima et al. 2000), highly suggestive of an accretion disk.

In common with many other LLAGN, optical images reveal large quantities of dust in filamentary structures within the inner regions of NGC 3226 (e.g. Rest et al. 2001). The X-ray presented here also indicate intrinsic absorption. The equivalent hydrogen column density reported in §4.2 ($3\text{--}7 \times 10^{21} \text{ cm}^{-2}$) corresponds to $2 \lesssim A_V \lesssim 4$ assuming a Galactic dust-to-gas ratio. Using the spectral energy distributions of M 81 and NGC 4579 as templates, both of which have an optical-to-X-ray spectral index $\alpha_{ox} = -\log(f(2 \text{ keV})/f(250 \text{ nm}))/2.605 \simeq 1.0$ (after correcting for the better-known reddening in these galaxies), we predict the nucleus has $m_V \simeq m_R \gtrsim 21$. The nucleus is therefore predicted to be swamped by the stellar emission (Rest et al. find $\mu_R \sim 14 \text{ arcsec}^{-2}$) in the central regions, consistent with observations.

These characteristics strongly suggest NGC 3226 hosts a central AGN. Such an hypothesis is also consistent with the broad component to the $H\alpha$ emission line suggested by Ho et al. (1997b) based on modeling of a fairly noisy spectrum of the $H\alpha$ region (where $H\alpha$ is blended with [N II] and [S II]; see their Fig. 10a). Terashima, Ho & Ptak (2000) have reported a strong correlation between $L(2\text{--}10 \text{ keV})$ and the luminosity of $H\alpha$ for a number of galaxies containing type 1 LINERs. This correlation has recently been confirmed and extended by Ho et al. (2001). This correlation supports the hypothesis that the dominant ionization source of the type 1 LINERs is the photon field of a central LLAGN. NGC 3226 is consistent with this correlation, adding further support to this hypothesis. The fact that the observed broad component of $H\alpha$

¹¹ Due to the orientation of the grating arms and the dithering of the spacecraft during the observation the relationship between ACIS pixel and wavelength is complex and time-variable.

constitutes a lower fraction ($\sim 60\%$) of the total (broad plus narrow) line emission compared to a more “normal” Seyfert 1 galaxy (eg. $\sim 97\%$ in NGC 3516) suggests differential (probably patchy) absorption towards the narrow- and broad-line regions.

4.3.1. Constraints on the Accretion Process

The optical luminosity of the entire galaxy NGC 3226 ($M_{\text{BT}} = -19.4$; $L_{\text{B}}/L_{\odot} \simeq 8 \times 10^9$) and a central, line-of-sight velocity dispersion ($\simeq 180 \text{ km s}^{-1}$; Simien & Prugniel 1998) are consistent with the relation found for a variety of galaxies harboring black holes (eg Gebhardt et al. 2000a; and references therein). The implied central black hole mass is $\simeq 10^8 M_{\odot}$, and hence the implied accretion rate is $\dot{m} \sim 4 \times 10^{-6} h_{75}^{-1} f_{\text{bolX}} \dot{M}_{\text{Edd}}$, where f_{bolX} is the ratio of bolometric to 0.4–10 keV luminosity (which is unlikely to much exceed 10), and \dot{M}_{Edd} is the Eddington accretion rate. Some words of caution are necessary. First, we note that the line-of-sight velocity dispersion quoted above is derived from ground-based observations – as yet there have been no *HST* observations capable of resolving the central kinematics of NGC 3226. Second, there have recently been a number of questions raised regarding the exact relation between the luminosity of the bulge and the mass of the black hole estimated by various means in different samples (eg. see Gebhardt et al. 2000b; Merritt & Ferrarese 2001, and references therein). Nevertheless, if a black hole indeed exists at the center of NGC 3226, the accretion rate is surely $\dot{m} \lesssim 10^{-2} \dot{M}_{\text{Edd}}$.

In systems with such low rates, the mass infall is generally thought to occur via a “standard” (geometrically-thin, viscosity-dominated) accretion disk at large radii, but switch to a radiatively less-efficient advection-dominated accretion flow (ADAF) in the inner regions (e.g. Narayan, Mahadevan & Quataert 1998, and references therein). The transition radius at which the flow becomes advection-dominated depends on a number of model parameters. Estimates range from ~ 10 – 10^2 Schwarzschild radii for several LLAGN (including M 81 and NGC 4579; e.g. see Quataert et al. 1999) to $\sim 10^3$ Schwarzschild radii for giant elliptical galaxies within clusters (Di Matteo et al. 2000). The X-ray emission from ADAFs is believed to be dominated by thermal bremsstrahlung (with $kT \sim \text{few keV}$), and not expected to exhibit significantly variability on timescales shorter than the local dynamical time ($\sim 5 \times 10^4 \text{ s}$ at 10 Schwarzschild radii from a $10^8 M_{\odot}$ black hole – see also Ptak et al. 1998). In §4.2 we found a thermal bremsstrahlung model to be consistent with the observed spectrum of the nucleus. However, if the variability on timescales $\lesssim \text{few} \times 10^3 \text{ s}$ suggested in §4.1 is confirmed, time-dependent models will be required.

5. THE OFF-NUCLEAR SOURCES CXO J102334.1+195347 AND CXO J102326.7+195407

There are too few counts from either CXO J102334.1+195347 AND CXO J102326.7+195407 to enable detailed analysis. We find no evidence for statistically significant variability on any timescale. Nevertheless some crude insight can be gained from consideration of counts detected in different energy bands. For CXO J102334.1+195347, the ratio of source counts (0.3-2 keV)/(2–10 keV) = 0.84 ± 0.40 . For a power law spectrum, such a ratio can be obtained with

$0.9 \lesssim \Gamma \lesssim 1.8$ if absorption by only $N_{\text{HI}}^{\text{gal}}$ is assumed, or with $\Gamma = 2$ and additional absorption of $N_{\text{H}} \simeq 10^{21}$ – 10^{22} cm^{-2} . In the case of CXO J102326.7+195407, we find the ratio of counts (0.3-2 keV)/(2–10 keV) $\lesssim 0.2$, indicative of an even harder spectrum. Assuming absorption by only $N_{\text{HI}}^{\text{gal}}$, a power law with $\Gamma \lesssim 0.5$ is required. Assuming a power law with $\Gamma = 2$, additional absorption with $N_{\text{H}} \gtrsim 2 \times 10^{22} \text{ cm}^{-2}$ is required.

The proximity of both sources to the nucleus (within a projected distance $\sim 1.3 h_{75}^{-1} \text{ kpc}$) strongly suggests both are X-ray sources within NGC 3226. The observed flux from each source is $\sim \text{few} \times 10^{-14} \text{ erg cm}^{-2} \text{ s}^{-1}$ in the 2–10 keV band. The density of background sources is $\lesssim 10^2 \text{ deg}^{-2}$ in this band at this flux level (e.g. Mushotzky et al 2000; Tozzi et al. 2001; and references therein). Thus the probability of a background source this bright within 15 arcsec of the nucleus of NGC 3226 is $\lesssim 10^{-4}$.

Assuming both sources are indeed within NGC 3226, the spectral forms described above imply absorption-corrected luminosities in the range $\sim \text{few} \times 10^{38}$ – $\text{few} \times 10^{39} h_{75}^{-1} \text{ erg s}^{-1}$. Assuming all emission from each source is indeed due to a single object, either or both CXO J102334.1+195347 and CXO J102326.7+195407 therefore have luminosities exceeding the Eddington limit for neutron stars ($\sim 3 \times 10^{38} \text{ erg s}^{-1}$), and hence must be $\gtrsim \text{few} M_{\odot}$ black-holes, very young supernovae or micro-quasars. Such superluminal sources are now being found regularly by *CXO* (eg. Griffiths et al. 2000; Fabbiano, Zezas & Murray 2001). Variability and detailed X-ray spectroscopic studies are the most likely means the various source types can be distinguished.

6. CONCLUSIONS AND FUTURE PROSPECTS

The results presented here illustrate the power of X-ray observations to detect and characterize the emission from LLAGN: a class of source which can usually only otherwise be studied at radio wavelengths and possibly with high signal-to-noise, high-resolution optical emission-line studies. Indeed in many cases, as for NGC 3226, the nucleus is expected to be invisible to *HST* in the optical band. We anticipate that many such objects will be detected serendipitously in the fields of future *CXO* and *XMM-Newton* observations. These data will expand the regions of parameter space accessible to study, surely resulting in a better understanding of the AGN/black-hole phenomenon.

We thank Lorella Angelini, Mike Loewenstein and Raymond White III for useful discussions. We acknowledge the financial support of the Joint Center for Astrophysics (IMG, TJT), NASA (TJT, through grant number NAG5-7385 (LTSA)), and the Universities Space Research Association (KN). This research has made use of the Simbad database, operated by the Centre de Données astronomiques de Strasbourg (CDS); the *VizieR* Service for Astronomical Catalogues, developed by CDS and ESA/ESRIN; the Hypercat Extragalactic database, provided by the Centre de Recherche Astronomique de Lyon; the NASA/IPAC Extragalactic Database (NED), operated by the Jet Propulsion Laboratory, California Institute of

Technology, under contract with NASA; and of data obtained through the HEASARC on-line service, provided by NASA/GSFC.

REFERENCES

- Cotton, W.D., Condon, J.J., Arbizzani, E., 1999, *ApJS*, 125, 409
Di Matteo, T., Quataert, E., Allen, S.W., Narayan, R., Fabian, A.C., 2000, *MNRAS*, 311, 507
Fabbiano, G., Zezas, A., Murray, S.S., 2001, *ApJ*, in press (astro-ph/0102256)
Falcke, H., Nagar, N.M., Wilson, A.S., Ulvestad, J.S., 2000, *ApJ*, 542, 197
Gebhardt, K., et al., 2000a, *ApJ*, 539, L13
Gebhardt, K., et al., 2000b, *ApJ*, 543, L5
George, I.M., Yaqoob, T., Turner, T.J., Kraemer, S., Ptak, A., Crenshaw, D.M., Netzer, H., Mushotzky, R.F., Nandra, K., 2001, *ApJ*, in prep. (G01)
Griffiths, R.E., Ptak, A., Feigelson, E.D., Garmire, G., Townsley, L., Brandt, W.N., Sambruna, R., Bregman, J.N., 2000, *Science*, 290, 1325
Ho, L.C., 1999, *ApJ*, 516, 672
Ho, L.C., Filippenko, A.V., Sargent, W.L.W., 1997a, *ApJS*, 112, 315
Ho, L.C., Filippenko, A.V., Sargent, W.L.W., Peng, C.Y., 1997b, *ApJS*, 112, 391
Ho, L.C., et al. 2001, *ApJ*, 549, L51
Houck, J., 2000, MIT Center for Space Research Memorandum, 2000 Aug 01
Ishisaki, Y., et al., 1996, *PASJ*, 48, 237
Komossa, S., Fink, H., 1997, *A&A*, 327, 483
Markert, T. H., Canizares, C. R., Dewey, D., McGuirk, M., Pak, C. S., Schattenburg, M. L. 1994, *Proc. SPIE*, 2280, 168
Merritt, D., Ferrarese, L., 2001, *MNRAS*, 320, L30
Murphy, E.M., Lockman, F.J., Laor, A., Elvis, M., 1996, *ApJS*, 105, 369
Mushotzky, R.F., Cowie, L.L., Barger, A.J., Arnaud, K.A., 2000, *Nature*, 404, 459
Narayan, R., Mahadevan, R., & Quataert, E., 1998, in *The Theory of Black Hole Accretion Disks*, ed. M.A. Abramowicz, G. Björnsson, & J.E. Pringle (Cambridge: Cambridge Univ. Press)
Nagar, N.M., Falcke, H., Wilson, A.C., Ho, L.C., 2000, *ApJ*, 542, 186
Nousek, J.A., et al. 1998, *Proc. SPIE*, 3444, 225
Ptak, A., Yaqoob, T., Mushotzky, R.F., Serlemitsos, P., Griffiths, R., 1998, *ApJ*, 501, L37
Quataert, E., Di Mattao, T., Narayan, R., Ho, L.C., 1999, *ApJ*, 525, L89
Rest, A., van den Bosch, F.C., Jaffe, W., Tran, H., Tsvetanov, Z., Ford, H.C., Davies, J., Schafer, J., 2001, *AJ*, in press (astro-ph/0102286)
Roberts, T.P., Warwick, R.S., 2000, *MNRAS*, 315, 98
Sansom, A.E., Hibbard, J.E., Schweizer, F., 2000, *AJ*, 120, 1946
Simian, F., Prugniel, P., 1998, *A&AS*, 131, 287
Terashima, Y., Ho, L.C., Ptak, A.F., Yaqoob, T., Kunieda, H., Misaki, K., Serlemitsos, P.J., 2000, *ApJ*, 535, L79
Terashima, Y., Ho, L.C., Ptak, A.F., 2000, *ApJ*, 539, 161
Tozzi, P., et al., 2001, *ApJ*, submitted (astro-ph/0103014)
de Vaucouleurs, G., de Vaucouleurs, A., Corwin Jr., H.G., Buta, R.J., Paturel, G., Fouque, P., 1991, *Third Reference Catalogue of Bright Galaxies (version RC3.9)*
Weisskopf, M.C., O'Dell, S.L., van Speybroeck, L.P., 1996, *Proc. SPIE*, 2805